Pathol. Oncol. Res. (2012) 18:413–420
DOI 10.1007/s12253-011-9461-0

RESEARCH

Brevican, Neurocan, Tenascin-C and Versican are Mainly Responsible for the Invasiveness of Low-Grade Astrocytoma

Imre Varga · Gábor Hutóczki · Csaba D. Szemcsák · Gábor Zahuczky · Judit Tóth · Zsolt Adamecz · Annamária Kenyeres · László Bognár · Zoltán Hanzély · Almos Klekner

Received: 3 March 2011 / Accepted: 9 September 2011 / Published online: 14 October 2011

Abstract The extent of tumor removal determines the effectiveness of postoperative oncotherapy. This is especially true for primary brain tumors, where peritumoral invasion usually makes radical resection impossible. The aim of the study was to determinate the specific expression pattern of invasion related molecules of different intracranial tumors and to identify molecules that are principally responsible for the peritumoral invasiveness of grade II astrocytoma mRNA expression of 26 extracellular matrix (ECM) molecules was determined in tissue samples from grade II astrocytoma, schwannoma, intracerebral metastases of non-small cell lung cancer and normal brain. Immunohistochemical staining for brevican, neurocan, tenascin-C and versican was also performed for each tumor group. Comparing astrocytoma to metastasis, schwannoma and normal brain; and metastasis and schwannoma to normal brain, 22, 17, 20, 21, and 19 molecules, respectively, were found to be significantly overexpressed at the mRNA level. Cluster analysis of mRNA expression showed a specific gene expression pattern for each histological group. Four molecules of 26 were found to be associated to astrocytoma. Immunohistochemical staining confirmed the results of the mRNA analysis at the protein level. Tumors of different origin have a specific invasive phenotype that can evidently determinate on gene expression level. This characteristic expression pattern of the invasion-related molecules might help to screen exact targets for anti-invasion drugs. In case of low-grade astrocytoma. brevican, neurocan, tenascin-C and versican were found to correlate principally with the invasive phenotype of low-grade astrocytoma, thus these molecules can potentially serve as targets for anti-invasion therapy in the future.

Keywords Astrocytoma · Brain metastasis · Schwannoma · Normal brain · Extracellular matrix · Invasion

Abbreviations

BEHAB/Brevican	Brain Enriched Hyaluronan Binding/Brevican
ECAM	Endothelial Cell Adhesion Molecule
ECM	Extracellular Matrix

I. Varga
Department of Pulmonology, Kenézy Gyula Hospital,
Debrecen, Hungary

G. Hutóczki · C. D. Szemcsák · L. Bognár · A. Klekner (✉)
Department of Neurosurgery, MHSC, University of Debrecen,
4032 DebrecenNagyerdei krt. 98.,
Hungary
e-mail: aklekner@yahoo.com

G. Zahuczky
Department of Biochemistry and Molecular Biology, MHSC,
University of Debrecen,
Debrecen, Hungary

J. Tóth
Institute of Oncology, MHSC, University of Debrecen,
Debrecen, Hungary

Z. Adamecz
Department of Radiotherapy, MHSC, University of Debrecen,
Debrecen, Hungary

A. Kenyeres
Institute of Anatomy, MHSC, University of Debrecen,
Debrecen, Hungary

Z. Hanzély
National Institute of Neurological Sciences,
Budapest, Hungary

G. Zahuczky
UD-GenoMed Medical Genomic Technologies Ltd.,
Debrecen, Hungary

EGF	Epidermal Growth Factor
EGFR	Epidermal Growth Factor Receptor
GAG	Glucose Amino Glucane
GAPDH	Glyceraldehyde 3-Phosphate Dehydrogenase
GBM	Glioblastoma Multiform
GFAP	Glial Fibrillary Acidic Protein
HAS	Hyaluronan Synthase
HS	Heparan Sulfate
HSPG	Heparan Sulfate Proteoglykane
ICAM	Inter-Cellular Adhesion Molecule
MHC	Major Histocompatibility Complex
MMP	Matrix Metalloproteinase
NCAM	Neuronal Cell Adhesion Molecule
NSCLC	Non-Small-Cell-Lung-Cancer
PCAM	Platelet Cell Adhesion Molecule
PCR	Polymerase Change Reaction
PG	Proteoglycane
RT-QPCR	Real Time Quantitative PCR
TNC	Tenascin-C
VCAM	Vasculare Cell Adhesion Molecule
WHO	World Health Organization

Introduction

Therapeutic efficacy in brain tumors is mainly influenced by the tumors' capacity for peritumoral infiltration. Interestingly, there is extensive variability in the extent of invasion among intracerebral tumors of the same grade but different histology [1, 2]. Gliomas are well known to invade deeply into the surrounding brain tissue, and this invasiveness can also be observed in low-grade astrocytomas. Thus, radical removal of astrocytomas is a great challenge for neurosurgeons [3, 4]. In contrast, brain metastases of anaplastic and de-differentiated lung adenocarcinoma form spheroids that are well demarcated from the brain, and total extirpation of these metastases is a routine operation [5, 6].

Peritumoral infiltration is dependent on the interactions between tumor cells and molecules of the extracellular matrix (ECM) in the surrounding brain. Fibrils, glycosaminoglycans, proteoglycans, laminins, enzymes and many other components of the ECM comprise the group of molecules that is involved in the peritumoral infiltration process [7].

There are a considerable high number of ECM molecules that are described to influence the peritumoral invasion of brain tumors. To investigate the invasive feature of intracranial tumors of different origin the mRNA expression of a selected group of 26 ECM components were compared among normal brain, two tumors of neuroectodermal origin (astrocytoma and schwannoma) and intracerebral metastases of non-small cell lung cancer (NSCLC). The aim of the study was to determinate the specific expression pattern of invasion related molecules of different intracranial tumors and to identify molecules that are principally responsible for the peritumoral invasiveness of grade II astrocytoma.

Patients and Methods

Tissue Samples

Thirty-six tissue samples were collected during neurosurgical operations. The samples were frozen promptly after removal on the surface of liquid nitrogen and were stored at −80°C until processing. Each sample was collected from a different patient. The following were carefully selected by an experienced neuropathologist for further investigation: nine samples from grade II astrocytoma, ten samples from intracerebral NSCLC metastases, eight samples from intracranial schwannoma, and nine samples of normal brain tissue that were collected during functional neurosurgery for epilepsy. Only completely normal brain tissue was used for analysis; gliosis, cortical dysplasia and damaged tissues were closed out from the investigations. Sections for histological analysis and immunohistochemistry were cut from the same samples used for mRNA analysis. All procedures were approved by the National Ethical Committee, and every patient signed an informed consent form.

RNA Analysis

The mRNA expression of 26 ECM-related molecules was determined by real-time quantitative reverse transcriptase–polymerase chain reaction (RT–PCR); these included 22 ECM molecules, two different metalloproteinases (MMPs) and two hyaluronan synthases (HASs). The expression of tumor markers (glial fibrillary acidic protein [GFAP] and cytokeratins 18 and 19), the proliferation marker Ki-67 and glyceraldehyde 3-phosphate dehydrogenase (GAPDH) was also tested.

RNA analysis was performed as described previously [1, 2]. Specifically, fresh frozen tissue samples were first pulverized with a manual CryoPress device (Microtec Co., Ltd, Japan) pre-cooled in liquid nitrogen. The pulverized frozen tissue was then scraped into the appropriate volume of TriReagent (Invitrogen, USA) and homogenized instantly with a rotor-stator homogenizer. Total RNA was isolated from TriReagent lysates according to the manufacturer's instructions. RNA purity and quantity were assessed on a NanoDrop® ND-1000 Spectrophotometer (NanoDrop Technologies, USA) and then stored at −80°C. RNA quality

was checked on 1.2% agarose gels stained with ethidium bromide. Total RNA was converted to single-stranded cDNA using the High Capacity cDNA Archive Kit with RNasin (Applied Biosystems, USA) and 600 ng of total RNA per sample in one reverse transcription reaction. cDNA transcribed from 100 ng of total RNA was loaded into each port of the microfluidic card.

TaqMan Low Density Array (TLDA) experiments were performed using the Applied Biosystems 7900HT real-time PCR system with the Micro Fluidic Card upgrade (Applied Biosystems, USA). The Micro Fluidic Card format allowed the analysis of 31 genes per sample, and each sample was analyzed in duplicate. The Micro Fluidic Cards were analyzed with the SDS 2.1 software as relative quantification studies with automatic threshold settings, and the C_T values were exported for further analysis. Each 40-gene set contained the housekeeping GAPDH. GAPDH showed the least variation among the samples and was used as the reference gene to calculate the dCt value for each gene.

Expression values were calculated using the comparative C_T method, as described previously [8]. Briefly, assuming that the PCR efficiency for any gene on the TLDA is close to 1, mRNA expression [9] for a given gene in the tumor or normal (calibrator) sample can be compared using the following simplified equation [10]: $X_{tumor} = 2^{-dCTtumor}$ and $X_{normal} = 2^{-dCTnormal}$

2^{-dCT} values were inputted for further analysis with GeneSpring 7.3 software (Silicon Genetics, Redwood City CA, USA); this allowed inspection of individual mRNA expression (X) differences within sample categories.

Statistic Analysis

The Mann–Whitney *U* test was used to identify genes with significantly different expression levels between different sample group, and $p<0.05$ was considered statistically significant. For testing the specificity of mRNA expression patterns of distinct histological tissue groups, hierarchical clustering was performed using complete linkage analysis with Pearson correlation.

Histochemistry

After evaluating mRNA results, brevican, neurocan, tenascin-C and versican were selected for investigation at the protein level with immunohistochemistry.

Frozen samples were fixed in Saint Marie's fixative [11, 12] for 24 h at 4°C. After fixation and dehydration, the tissue samples were embedded in wax, and 5-μm sections were cut. The sections were stained with hematoxylin–eosin, and immunohistochemical reactions were carried out according to the following protocol. Slides were pre-incubated in ready-to-use 2.5% normal horse serum (Vector, Burlingame, CA, USA) for 30 min at 37°C to prevent nonspecific binding of primary antibodies. For determination of brevican MAB40091 (R&D Systems, Minneapolis, USA), of neurocan AB26003 (ABCAM, Cambridge, USA), of tenascin AB19011, and of versican AB1032 (Chemicon, Millipore, USA) was used. Ki-67, GFAP, CK-18 and 19 was tested by MAB4190, AB5804, MAB1600 and MAB3238 (Chemicon, Millipora, USA) respectively. The sections were then incubated overnight at 4°C with the appropriately diluted antibodies. For morphological examinations, immunohistochemical and hemalaun staining were performed on additional sections. The immunohistochemical reactions were visualized with the avidin–biotin–peroxidase complex, and the peroxidase was detected with a solution containing the H_2O_2 substrate and the diaminobenzidine (DAB) chromogen (ImmPress Reagent Kit, Vector; Peroxidase Substrate DAB Kit, Vector). Finally, the nuclei were labeled with hemalaun staining, and the sections were mounted in DePeX (BDH Laboratory Supplies, Poole, UK). To control for the specificity of the immunohistochemical reactions, sections were treated with the same protocol, excluding the primary antibodies, which were replaced with nonimmune IgG (Sigma, St Louis, MO, USA) solution at the optimal dilution for the different primary antibodies.

Immunohistochemistry results were evaluated by three different investigators experienced in histology and scored from 1 to 3. Morphological evaluations were conducted separately.

Results

RNA Analysis

Upon comparison of gene expression between NSCLC brain metastases and grade II astrocytoma, the expression of cadherin-3, collagen type I, III and IV, fibronectin, perlecan, syndecan-1 and −4 and MMP-9 was found to be significantly higher in metastasis samples. In contrast, the expression of brevican, cadherin-2, laminin alpha-4 and beta-2, matrillin-2, neurocan, neuroglycan-C, syndecan-3, tenascin-C and -R, versican, HAS-2, and MMP-2 was found to be higher in astrocytoma tissues.

NSCLC brain metastases also had elevated mRNA levels of cadherin-3, neurocan, syndecan-1 and MMP-9 compared to schwannoma tissues, whereas schwannoma tissues had higher expression of cadherin-2, collagen type IV and VIII, laminin alpha-4, beta-1 and beta-2, matrillin-2, neuroglycan-C, perlecan, syndecan-3, HAS-2 and MMP-2.

Upon comparison of schwannoma and astrocytoma samples, the expression of collagen type I alpha-1, collagen type III, IV and VIII, fibronectin, perlecan, matrillin-2,

syndecan-4, laminin alpha-4, beta-1 and beta-2 was found to be increased in schwannoma tissues, whereas brevican, neuroglycan-C, tenascin-C and -R, neurocan and versican were found to be more highly expressed in astrocytoma tissues.

Comparison of astrocytoma samples to normal brain samples revealed that mRNA levels of agrin, brevican, cadherin-2, collagen type I, III and IV, fibronectin-1, laminin alpha-4 and beta-2, matrillin-2, neurocan, perlecan, syndecan-3, tenascin-C, versican, HAS-2, and MMP-2 were significantly higher in astrocytoma samples. In contrast, syndecan-4 and HAS-1 mRNA levels were higher in normal brain tissues.

Schwannoma samples had higher mRNA levels of agrin, collagen types I, III IV and VIII, fibronectin, laminin alpha-4, beta-1 and beta-2, matrillin-2, perlecan, syndecan-3 and −4, HAS-2 and MMP-2 when compared to normal brain samples, while normal brain samples had higher mRNA levels of brevican, neurocan, neuroglycan-C and tenascin-R.

The expression of agrin, cadherin-3, collagen type I, III, IV and VIII, fibronectin, laminin beta-1 and beta-2, perlecan, syndecan-1 and −4 and MMP-9 was significantly higher in brain metastases than in normal brain. In contrast, the expression of brevican, cadherin-2, neurocan, neuroglycan-C, matrillin-2, syndecan-3, tenascin-R and HAS-1 was significantly lower in metastases than in normal brain tissue.

Histochemistry

Immunoreactivity for brevican, neurocan, tenascin-C and versican was most intense mainly in the tumor stroma especially around capillaries and small vessels. The strongest immunohistochemical staining for all molecules was observed in astrocytoma tissues. Normal brain tissues had weaker immunostaining for neurocan, tenascin-C and versican, and schwannoma samples had even weaker immunostaining for brevican and neurocan. Metastatic tissues exhibited the weakest immunostaining for versican. Tenascin-C staining was very weak in both schwannoma and NSCLC tissues. The staining intensity of tumor markers and Ki-67 was in accordance with the histological diagnosis.

Discussion

The extent of tumor removal determines the effectiveness of postoperative oncotherapy. This is especially true for primary brain tumors, where peritumoral invasion usually makes radical resection impossible. Peritumoral infiltration is observed not only in malignant gliomas but also in low-grade tumors, such as grade II astrocytoma [13–16]. Interestingly, brain metastases of NSCLC are only moderately invasive such that radical extirpation is generally a routine neurosurgical procedure [5, 17, 18].

The presence of each ECM compartment in different tumors can be found in the literature (detailed below), but simultaneous analysis of a wide spectrum of molecules selected by one specific feature, like invasion of brain tumors was not reported until now. The aim of the study was firstly to determinate and compare the expression pattern of invasion related ECM molecules of intracranial tumors of different origin and secondly to identify molecules that are principally responsible for the peritumoral invasiveness of grade II astrocytoma. Because tumor invasion is highly dependent on interactions between a considerable great number of ECM components and tumor cells, we examined the gene expression of a selected group of 26 ECM molecules that have previously been reported to actively participate in peritumoral infiltration.

The gene expression was investigated in tissue samples from the infiltrative semi-benign grade II astrocytoma, the non-infiltrative and benign schwannoma, and the non-infiltrative but malignant brain metastasis of NSCLC. By determining the mRNA expression of 26 invasion-related molecules, an mRNA expression pattern was created for each group. Cluster analysis was used to test the specificity of changes in the expression pattern of these molecules (Fig. 1). Due to this statistical test it can be evidently established that each tissue group has a characteristic expression pattern of these invasion-related molecules indicating that the mRNA expression pattern of these 26 molecules might be a specific feature of the tumor tissue.

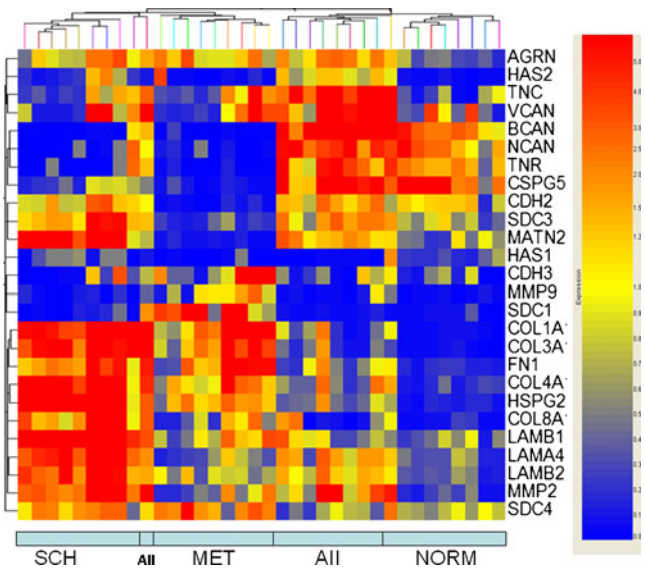

Fig. 1 Hierarchical clustering with complete linkage analysis with Pearson correlation for testing the specificity of mRNA expression pattern of 26 invasion-related ECM molecules in normal brain (NORM), grade II astrocytoma (A II), intracerebral adenocarcinoma metastasis (MET) and schwannoma (SCH)

The expression of brevican, neurocan, neuroglycan-C, tenascins, versican and MMP-2 was characteristic for normal brain and grade II astrocytoma, while the ECM of schwannoma and adenocarcinoma contained predominantly collagens, fibronectin, syndecans, laminins and cadherins. These specific ECM profiles indicates the high ratio of connective tissue in shwannoma and metastasis, while gliotic tissues express their own characterisctic GAGs and PGs (Fig. 1). This similarity of astrocytoma grade II and normal brain can explain the extent migration of glioma cells into the surrounding brain tissue and the significant difference between adenocarcinoma and normal brain helps to understand the reduced effectiveness of intracerebral peritumoral infiltration.

To identify molecules that are mainly responsible for invasiveness of grade II astrocytoma, gene expression results were also compared one by one among tumor groups and normal brain tissue. First, astrocytoma samples were compared to metastasis samples, and we found thirteen molecules that were expressed significantly higher in astrocytoma (Table 1). By comparing these thirteen molecules between metastasis samples and schwannoma samples we found eight molecules that showed significantly elevated expression in schwannoma (cadherin-2, neuroglycan-C, laminin alpha-4, laminin beta-2, matrillin-2, syndecan-3, HAS-2 and MMP-2). As neither tumor is infiltrative the differential expression of these eight molecules is probably because of the different cytogenetic origins and they can suppose to be unrelated to the invasive phenotype. Falling out these eight molecules, the reminders were compared between astrocytoma and schwannoma samples. The mRNA levels of the five molecule (brevican, neurocan, tenascin-C, -R and versican) were found to be significantly elevated in astrocytoma. Finally, these five molecules were tested again in case of astrocytoma and normal brain: the expression of four molecules (brevican, neurocan, tenascin-C and versican) was significantly increased in astrocytoma (Fig. 2). Astrocytoma samples showed different expression of sixteen additional molecules compared to normal brain tissue, but the analysis did not proved any positive correlation between elevated expression of these molecules and invasive potential of the

Table 1 Comparison of mRNA expression of 26 invasion-associated ECM molecules in normal brain (NRM), cerebral metastasis of NSCLC (MET), grade II astrocytoma (AII) and schwannoma (SCH). (*FC* fold change: it was calculated by dividing the relative gene expression levels in given samples as indicated in the cells; *P p* value; - = $p>0.05$; + = $p\leq0.05$; ++ = $p\leq0.01$). Significant differences are in bold.

	FC NRM/MET	P	FC MET/AII	P	FC MET/SCH	P	FC NRM/AII	P	FC SCH/AII	P	FC NRM/SCH	P
agrin	**0.31**	++	0.88	−	0.99	−	**0.27**	++	0.89	−	**0.30**	++
brevican	**20.32**	++	**0.01**	++	13.48	−	**0.13**	+	**0.001**	++	**273.94**	++
cadherin-2	**6.29**	++	**0.10**	++	**0.10**	++	**0.60**	+	0.99	−	0.61	−
cadherin-3	**0.12**	+	**7.50**	+	**5.05**	+	0.91	−	1.48	−	0.61	−
collagen type I alpha-1	**0.02**	++	**4.24**	+	0.76	−	**0.08**	+	**5.60**	++	**0.01**	++
collagen type III alpha-1	**0.01**	++	**3.18**	+	0.45	−	**0.04**	++	**7.02**	++	**0.01**	++
collagen type IV alpha-1	**0.15**	++	**2.41**	+	**0.24**	++	**0.36**	+	**10.14**	++	**0.04**	++
collagen type VIII alpha-1	**0.18**	++	1.54	−	**0.14**	+	0.28	−	**11.35**	++	**0.02**	++
neuroglycan-C	**32.84**	++	**0.02**	++	**0.28**	++	0.75	−	**0.08**	++	**9.31**	++
fibronectin	**0.07**	++	**5.10**	+	1.21	−	**0.34**	+	**4.21**	++	**0.08**	++
hyaluronan-synthase-1	**22.12**	++	1.23	−	0.18	−	**27.18**	++	6.97	−	3.90	−
hyaluronan-synthase-2	0.33	−	**0.45**	++	**0.67**	+	**0.15**	++	0.68	−	**0.22**	++
perlecan	**0.10**	++	**2.63**	++	**0.06**	++	**0.26**	++	**45.58**	++	**0.01**	++
laminin alpha-4	0.76	−	**0.36**	++	**0.07**	++	**0.27**	++	**5.34**	++	**0.05**	++
laminin beta-1	**0.32**	+	1.09	−	**0.06**	++	0.35	−	**19.21**	++	**0.02**	++
laminin beta-2	**0.50**	+	**0.59**	+	**0.16**	++	**0.29**	++	**3.68**	++	**0.08**	++
matrillin-2	**4.31**	++	**0.08**	++	**0.01**	++	**0.36**	++	**7.05**	++	**0.05**	++
matrix-metalloproteinase-2	0.58	−	**0.47**	+	**0.12**	++	**0.27**	++	4.04	−	**0.07**	++
matrix-metalloproteinase-9	**0.09**	++	**6.68**	++	**12.30**	++	0.58	−	0.54	−	1.08	−
neurocan	**17.89**	++	**0.03**	++	**24.99**	++	**0.59**	++	**0.00**	++	**447.06**	++
syndecan-1	**0.02**	++	**80.73**	++	**40.51**	++	1.35	−	1.99	−	0.68	−
syndecan-3	**2.16**	+	**0.19**	++	**0.12**	++	**0.41**	++	1.62	−	**0.25**	++
syndecan-4	**0.33**	+	**5.32**	++	1.36	−	**1.78**	+	**3.91**	++	**0.45**	++
tenascin-C	2.11	−	**0.27**	++	3.00	−	**0.57**	++	**0.09**	++	6.35	−
tenascin-R	**12.16**	++	**0.04**	++	59.44	−	0.48	−	**0.00**	++	**723.00**	++
Versican	1.67	−	**0.11**	+	0.51	−	**0.18**	+	**0.22**	+	0.84	−

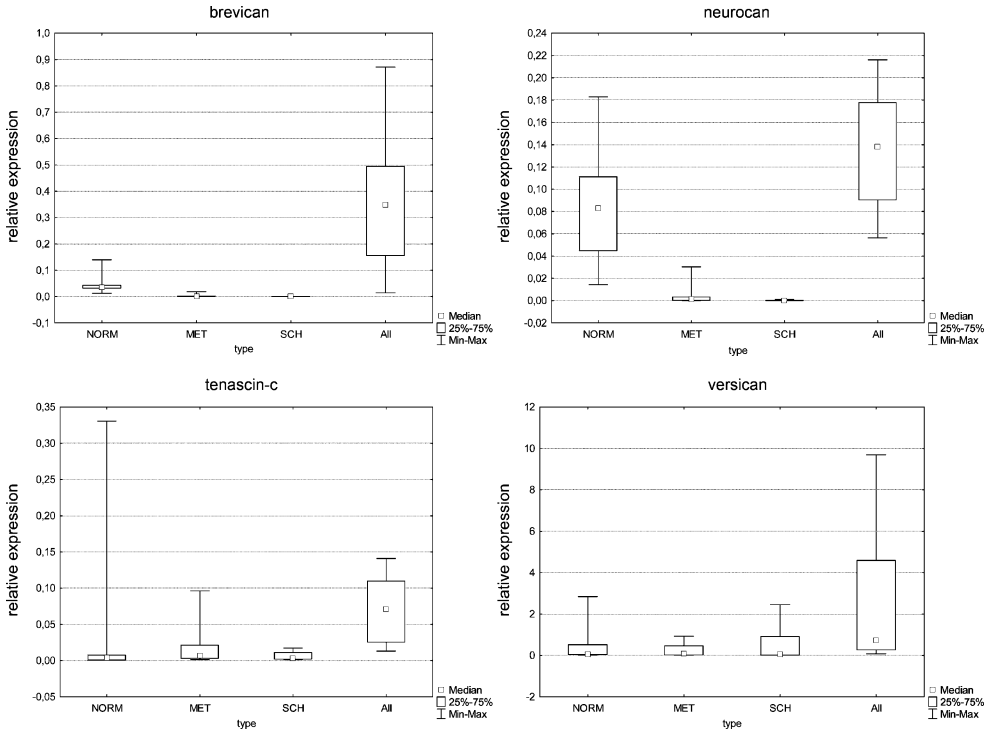

Fig. 2 Statistical analysis of mRNA expression of brevican, neurocan, tenascin-C and versican in normal brain (NORM), intracerebral metastasis of lung adenocarcinoma (MET), schwannomas (SCH) and astrocytoma grade II (AII)

investigated tumors. The mRNA expression of the four molecules identified at the end of the tests was not significantly higher in schwannoma or metastasis compared them to normal brain, which also supports their unique role in the peritumoral invasion of astrocytomas.

These four molecules have also been previously linked to peritumoral infiltration. Upregulation and cleavage of the brain-specific proteoglycan BEHAB/brevican has been shown to promote glioma invasion [19–22]. Brevican expression is upregulated during glial cell proliferation and/or motility, including during early central nervous system development and in invasive glioma [23–26]. At the molecular level, brevican promotes epidermal growth factor receptor (EGFR) activation, increases the expression of cell adhesion molecules, and promotes the secretion of fibronectin and accumulation of fibronectin microfibrils on the cell surface. Moreover, the N-terminal cleavage product of brevican, but not the full-length protein, associates with fibronectin in cultured cells and in surgical samples of glioma [19].

Neurocan is a major brain chondroitin sulfate proteoglycan that interacts with heparan sulfate proteoglycans (HSPGs) such as syndecan-3 and glypican-1 and is thought to modulate cell adhesion and migration [27–29]. The C-terminal fragment of neurocan, but not the N-terminal fragment, significantly increases the rate of neurite outgrowth in cultured cells. HSPGs such as syndecan-3 and glypican-1 are cell surface receptors for neurocan, and interactions between these HSPGs and the C-terminal domain of neurocan promotes neurite outgrowth [28].

The hexameric ECM glycoprotein tenascin is transiently expressed in many developing organs and is often re-expressed in tumors. It is present in the central and peripheral nervous systems as well as in smooth muscle and tendons [30–32]. Tenascin contains epidermal growth factor (EGF)-like domains and fibronectin-like repeats, which is consistent with its growth-promoting properties [33, 34]. It also has an anti-adhesive effect in many cell types [35]. Tenascin-C has been linked in vitro and in vivo to astrocytoma aggressiveness and invasion [36, 37]. Tenascin-C is also an independent prognostic indicator; its expression is enhanced in grade II astrocytomas, and positive tenascin-C expression is associated with a higher risk of recurrence [37]. In schwannomas, the tumor cells are tenascin-C-negative, whereas in more than half of the tumors, the vessels and ECM of regressively altered tumor areas are tenascin-C-positive. In metastatic carcinomas, the tumor cells are tenascin-C-negative; some vessels are tenascin-C-positive, which suggests that tenascin-C plays a role in angiogenesis [38]. Focal areas of the ECM, which often undergo fibrotic changes, are immunopositive for tenascin-C. The most constant tenascin-C immunoreactivity has been noted in the ECM of the fibrotic stroma of highly malignant brain tumors and along the tumor border, especially in high-grade astrocytoma [39–41].

Versican is a hyaluronan-containing proteoglycan found in the ECM of a variety of tissues and organs. It accumulates both in tumor stroma and cancer cells [42] and it participates in cell adhesion, migration, and

angiogenesis, which are all features of invasion and metastasis [1, 2]. Versican is one of the major ECM proteins in the brain. ECM molecules and their cleavage products critically regulate the growth and arborization of neurites, hence modulating the formation of neural networks [43, 44]. Peptide fragments containing the versican C terminus (G3 domain) are present in human brain astrocytoma. The versican G3 domain regulates neuronal attachment, neurite outgrowth, and synaptic function of hippocampal neurons via EGFR-dependent and -independent signaling pathway(s). In addition, the G3 domain has been reported to intensify dendritic spines [43]. Expression of a versican G3 construct in astrocytoma cells enhances colony growth, tumor growth and blood vessel formation. G3-containing medium enhances endothelial cell adhesion, proliferation, and migration [43, 45–47]. The expression of versican in NSCLC can be observed in both tumor stroma and cancer cells [48, 49]. High stromal versican staining correlates with poor disease-free survival, higher tumor recurrence rate and more advanced disease [2, 49]. For adenocarcinomas, high stromal staining of versican is associated with tumor recurrence, higher tumor stage and lymph node metastases [49].

Because many molecules are known to participate in glioma invasion, it is not easy to select targets for anti-invasion therapy. Our comparison of the expression pattern of various ECM molecules in tumors of different grade and invasion potential could help narrow down the number of target molecules.

Immunohistochemical results confirmed the high protein levels of brevican, neurocan, tenascin-C and versican in astrocytoma. These proteins were also detected in normal brain tissues but were very lowly expressed in schwannoma and metastasis tissues, which did not allow for a precise comparison between these tissues.

Conclusions

The mRNA expression pattern of these invasion-related molecules was highly specific for the tested histological groups. Thus, determination of the genetic signature of invasion of a tissue sample might help in screening exact molecules playing predominant role in the invasiveness of the actual tumor.

After comparing the expression of 26 invasion-related ECM components in infiltrating glioma, non-infiltrating malignant and benign tumors and normal brain brevican, neurocan, tenascin-C and versican were found to be associated with astrocytoma. Our analysis suggests that these molecules might be responsible for the invasive behavior of low-grade astrocytoma and could serve as potential targets for anti-invasive chemotherapy.

Conflict of Interest The authors report no conflict of interest concerning the materials or methods used in this study or the findings specified in this paper.

Financial Support This study was supported by the Hungarian Ministry of Education (OTKA, no. F-049050).

References

1. Klekner A, Varga I, Bognár L et al (2010) Extracellular matrix of cerebral tumors with different invasiveness. Ideggyogy Sz 63(1–2):38–43 (Hu)
2. Varga I, Hutóczki G, Petrás M et al (2010) Expression of invasion-related extracellular matrix molecules in human glioblastoma versus intracerebral lung adenocarcinoma metastasis. Cen Eur Neurosurg 71(4):173–180
3. Kyoshima K, Akaishi K, Tokushige K et al (2004) Surgical experience with resection en bloc of intramedullary astrocytomas and ependymomas in the cervical and cervicothoracic region. J Clin Neurosci 11(6):623–628
4. Ramina R, Coelho Neto M, Fernandes YB et al (2005) Intrinsic tectal low grade astrocytomas: is surgical removal an alternative treatment? Long-term outcome of eight cases. Arq Neuropsiquiatr 63(1):40–45
5. Abacioglu U, Caglar H, Atasoy BM et al (2010) Gamma knife radiosurgery in non small cell lung cancer patients with brain metastases: treatment results and prognostic factors. J BUON 15 (2):274–280
6. Catinella FP, Kittle CF, Faber LP et al (1989) Surgical treatment of primary lung cancer and solitary intracranial metastasis. Chest 136(5 Suppl):e30
7. Okada Y (2000) Tumor cell-matrix interaction: pericellular matrix degradation and metastasis. Verh Dtsch Ges Pathol 84:33–42
8. Livak KJ, Schmittgen TD (2001) Analysis of relative gene expression data using real-time quantitative PCR and the 2(−Delta Delta C(T)) method. Methods 25:402–408
9. Han S, Sidell N, Roman J (2005) Fibronectin stimulates human lung carcinoma cell proliferation by suppressing p21 gene expression via signals involving Erk and Rho kinase. Canc Lett 219(1):71–81
10. Hirose J, Kawashima H, Yoshie O et al (2001) Versican interacts with chemokines and modulates cellular responses. J Biol Chem 276(7):5228–5234
11. Sainte-Marie G (1962) A paraffin embedding technique for studies employing immunofluorescence. J Histochem Cytochem 10:250–256
12. Tuckett F, Morriss-Kay G (1988) Alcian blue staining of glycosaminoglycans in embryonic material: effect of different fixatives. Histochem J 20:174–182
13. Kono K, Inoue Y, Nakayama K et al (2001) The role of diffusion-weighted imaging in patients with brain tumors. AJNR Am J Neuroradiol 22(6):1081–1088
14. Lu S, Ahn D, Johnson G et al (2004) Diffusion-tensor MR imaging of intracranial neoplasia and associated peritumoral edema: introduction of the tumor infiltration index. Radiology 232(1):221–228
15. Miklós P, Gábor H, Imre V et al (2009) Expression pattern of invasion-related molecules in brain tumors of different origin. Magy Onkol 53(3):253–258 (Hu)
16. Wang W, Steward CE, Desmond PM (2009) Diffusion tensor imaging in glioblastoma multiforme and brain metastases: the role of p, q, L, and fractional anisotropy. AJNR Am J Neuroradiol 30 (1):203–208

17. Lo CK, Yu CH, Ma CC et al (2010) Surgical management of primary non-small-cell carcinoma of lung with synchronous solitary brain metastasis: local experience. Hong Kong Med J 16(3):186–191
18. Pfannschmidt J, Dienemann H (2010) Surgical treatment of oligometastatic non-small cell lung cancer. Lung Canc 69 (3):251–258
19. Hu B, Kong LL, Matthews RT et al (2008) The proteoglycan brevican binds to fibronectin after proteolytic cleavage and promotes glioma cell motility. J Biol Chem 283(36):24848–24859
20. Viapiano MS, Bi WL, Piepmeier J et al (2005) Novel tumor-specific isoforms of BEHAB/brevican identified in human malignant gliomas. Canc Res 65(15):6726–6733
21. Viapiano MS, Hockfield S, Matthews RT (2008) BEHAB/brevican requires ADAMTS-mediated proteolytic cleavage to promote glioma invasion. J Neurooncol 88(3):261–272
22. Viapiano MS, Matthews RT, Hockfield S (2003) A novel membrane-associated glycovariant of BEHAB/brevican is up-regulated during rat brain development and in a rat model of invasive glioma. J Biol Chem 278(35):33239–33247
23. Nutt CL, Matthews RT, Hockfield S (2001) Glial tumor invasion: a role for the upregulation and cleavage of BEHAB/brevican. Neuroscientist 7(2):113–122
24. Gary SC, Hockfield S (2000) BEHAB/brevican: an extracellular matrix component associated with invasive glioma. Clin Neurosurg 47:72–82
25. Gary SC, Kelly GM, Hockfield S (1998) BEHAB/brevican: a brain-specific lectican implicated in gliomas and glial cell motility. Curr Opin Neurobiol 8(5):576–581
26. Gary SC, Zerillo CA, Chiang VL et al (2000) cDNA cloning, chromosomal localization, and expression analysis of human BEHAB/brevican, a brain specific proteoglycan regulated during cortical development and in glioma. Gene 256(1–2):139–147
27. Talts U, Kuhn U, Roos G et al (2000) Modulation of extracellular matrix adhesiveness by neurocan and identification of its molecular basis. Exp Cell Res 259(2):378–388
28. Akita K, Toda M, Hosoki Y et al (2004) Heparan sulphate proteoglycans interact with neurocan and promote neurite outgrowth from cerebellar granule cells. Biochem J 383(Pt 1):129–138
29. Rauch U, Feng K, Zhou XH (2001) Neurocan: a brain chondroitin sulfate proteoglycan. Cell Mol Life Sci 58(12–13):1842–1856
30. Zinovieva E, Lebrun N, Letourneur F et al (2008) Lack of association between Tenascin-C gene and spondyloarthritis. Rheumatology (Oxford) 47(11):1655–1658
31. Meloty-Kapella CV, Degen M, Chiquet-Ehrismann R et al (2006) Avian tenascin-W: expression in smooth muscle and bone, and effects on calvarial cell spreading and adhesion in vitro. Dev Dyn 235(6):1532–1542
32. Pajala A, Melkko J, Leppilahti J et al (2009) Tenascin-C and type I and III collagen expression in total Achilles tendon rupture. Histol Histopathol 24(10):1207–1211
33. Engel J (1989) EGF-like domains in extracellular matrix proteins: localized signals for growth and differentiation? FEBS Lett 251 (1–2):1–7
34. Swindle CS, Tran KT, Johnson TD et al (2001) Epidermal growth factor (EGF)-like repeats of human tenascin-C as ligands for EGF receptor. J Cell Biol 154(2):459–468
35. Fischer D, Brown-Lüdi M, Schulthess T et al (1997) Concerted action of tenascin-C domains in cell adhesion, anti-adhesion and promotion of neurite outgrowth. J Cell Sci 110(Pt 13):1513–1522
36. Hirata E, Arakawa Y, Shirahata M et al (2009) Endogenous tenascin-C enhances glioblastoma invasion with reactive change of surrounding brain tissue. Canc Sci 100(8):1451–1459
37. Maris C, Rorive S, Sandras F et al (2008) Tenascin-C expression relates to clinicopathological features in pilocytic and diffuse astrocytomas. Neuropathol Appl Neurobiol 34(3):316–329
38. Bicer A, Guclu B, Ozkan A et al (2010) Expressions of angiogenesis associated matrix metalloproteinases and extracellular matrix proteins in cerebral vascular malformations. J Clin Neurosci 17(2):232–236
39. Kim CH, Bak KH, Kim YS et al (2000) Expression of tenascin-C in astrocytic tumors: its relevance to proliferation and angiogenesis. Surg Neurol 54(3):235–240
40. Leins A, Riva P, Lindstedt R et al (2003) Expression of tenascin-C in various human brain tumors and its relevance for survival in patients with astrocytoma. Cancer 98(11):2430–2439
41. Zagzag D, Capo V (2002) Angiogenesis in the central nervous system: a role for vascular endothelial growth factor/vascular permeability factor and tenascin-C. Common molecular effectors in cerebral neoplastic and non-neoplastic "angiogenic diseases". Histol Histopathol 17(1):301–321
42. Mukaratirwa S, Chimonyo M, Obwolo M et al (2004) Stromal cells and extracellular matrix components in spontaneous canine transmissible venereal tumour at different stages of growth. Histol Histopathol 19(4):1117–1123
43. Xiang YY, Dong H, Wan Y et al (2006) Versican G3 domain regulates neurite growth and synaptic transmission of hippocampal neurons by activation of epidermal growth factor receptor. J Biol Chem 281(28):19358–19368
44. Wu Y, Sheng W, Chen L et al (2004) Versican V1 isoform induces neuronal differentiation and promotes neurite outgrowth. Mol Biol Cell 15(5):2093–2104
45. Ricciardelli C, Sakko AJ, Ween MP et al (2009) The biological role and regulation of versican levels in cancer. Canc Metastasis Rev 28(1–2):233–245
46. Wu Y, Zhang Y, Cao L et al (2001) Identification of the motif in versican G3 domain that plays a dominant-negative effect on astrocytoma cell proliferation through inhibiting versican secretion and binding. J Biol Chem 276(17):14178–14186
47. Zheng PS, Wen J, Ang LC et al (2004) Versican/PG-M G3 domain promotes tumor growth and angiogenesis. FASEB J 18 (6):754–756
48. Soltermann A, Tischler V, Arbogast S (2008) Prognostic significance of epithelial-mesenchymal and mesenchymal-epithelial transition protein expression in non-small cell lung cancer. Clin Canc Res 14(22):7430–7437
49. Pirinen R, Leinonen T, Böhm J et al (2005) Versican in nonsmall cell lung cancer: relation to hyaluronan, clinicopathologic factors, and prognosis. Hum Pathol 36(1):44–50